Nanoplastics impaired oyster free living stages, gametes and embryos

Kevin Tallec, Arnaud Huvet, Carole Di Poi, Carmen González-Fernández, Christophe Lambert, Bruno Petton, Nelly Le Goïc, Mathieu Berchel, Philippe Soudant, Ika Paul-Pont

Environmental Pollution
November 2018, Volume 242, Part B, Pages 1226-1235
http://dx.doi.org/10.1016/j.envpol.2018.08.020
http://archimer.ifremer.fr/doc/00453/56419/

Nanoplastics impaired oyster free living stages, gametes and embryos

Tallec Kevin [1, *], Huvet Arnaud [1], Di Poi Carole [1], González-Fernández Carmen [2], Lambert Christophe [2], Petton Bruno [1], Le Goïc Nelly [2], Berchel Mathieu [3], Soudant Philippe [2], Paul-Pont Ika [2]

[1] Ifremer, Laboratoire des Sciences de l'Environnement Marin (LEMAR), UMR 6539 UBO/CNRS/IRD/Ifremer, CS 10070, 29280, Plouzané, France
[2] Laboratoire des Sciences de l'Environnement Marin (LEMAR), UMR 6539 CNRS/UBO/IRD/Ifremer – Institut Universitaire Européen de la Mer, Technopôle Brest-Iroise – Rue Dumont d'Urville, 29280, Plouzané, France
[3] Université de Brest, Université Européenne de Bretagne, CNRS UMR 6521, CEMCA, IFR 148 ScInBios, 6 Avenue Victor Le Gorgeu, 29238, Brest, France

* Corresponding author : Kevin Tallec, email address : kevin.tallec@univ-brest.fr

Abstract :

In the marine environment, most bivalve species base their reproduction on external fertilization. Hence, gametes and young stages face many threats, including exposure to plastic wastes which represent more than 80% of the debris in the oceans. Recently, evidence has been produced on the presence of nanoplastics in oceans, thus motivating new studies of their impacts on marine life. Because no information is available about their environmental concentrations, we performed dose-response exposure experiments with polystyrene particles to assess the extent of micro/nanoplastic toxicity. Effects of polystyrene with different sizes and functionalization (plain 2-µm, 500-nm and 50-nm; COOH-50 nm and NH2-50 nm) were assessed on three key reproductive steps (fertilization, embryogenesis and metamorphosis) of Pacific oysters (Crassostrea gigas). Nanoplastics induced a significant decrease in fertilization success and in embryo-larval development with numerous malformations up to total developmental arrest. The NH2-50 beads had the strongest toxicity to both gametes (EC50 = 4.9 µg/mL) and embryos (EC50 = 0.15 µg/mL), showing functionalization-dependent toxicity. No effects of plain microplastics were recorded. These results highlight that exposures to nanoplastics may have deleterious effects on planktonic stages of oysters, presumably interacting with biological membranes and causing cyto/genotoxicity with potentially drastic consequences for their reproductive success.

Graphical abstract

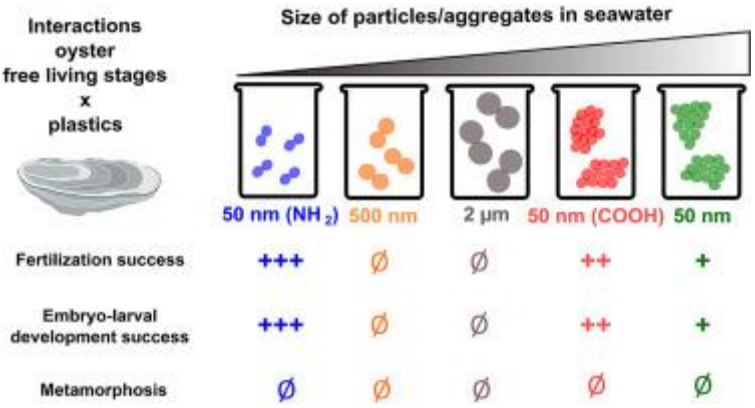

Highlights

► Oyster gametes, embryos and larvae were exposed to nano- and microplastics. ► Nanoplastics caused significant decrease in fertilization and embryogenesis success. ► Nanoplastics functionalization influences their behavior and toxicity. ► No effect of plain microplastics was demonstrated on all endpoints.

Keywords : Oyster, Embryos, Gametes, Microplastics, Nanoplastics

Introduction

Mismanagement of plastic wastes is one of the major concerns of the scientific community in the 21st century (Galloway et al., 2017). The exponential use of plastics by human society since 1950 has led to a significant release of wastes into the environment (Cole et al., 2011; Geyer et al., 2017). Between 13,200 and 34,800 tons of plastic debris were estimated to have been introduced daily into the oceans in 2010, and this amount is expected to increase by an order of magnitude by 2025 (Jambeck et al., 2015). Today, plastic debris are widespread and ubiquitous in marine environments from the sea surface (Eriksen et al., 2014) to the sediment (Van Cauwenberghe et al., 2015), including in remote areas such as polar regions (Cózar et al., 2017), deep-sediments (Bergmann et al., 2017) and desert islands (Lavers and Bond, 2017).

Microplastics (MP) are defined as particles with a size less than 5 mm (Galloway et al., 2017), originating from manufactured beads/fibers (primary MP) or weathering of larger waste (secondary MP). They represent the most abundant plastic items in oceans in terms of the number of particles per unit of water (>92% of floating plastics) (Cole et al., 2011; Eriksen et al., 2014). Recently, a new class of debris was described, namely nanoplastics (NP), defined as particles <100 nm (Galloway et al., 2017) or <1000 nm (Gigault et al., 2018). The definition used in the present study (<100 nm) refers to the usual definition of nanoscale; *i.e*. the point where the properties of a material change (higher surface area effect and interaction with biological membranes) (Klaine et al., 2012). Their production has been demonstrated by mechanical fragmentation (Lambert and Wagner, 2016), photo-degradation (Gigault et al., 2016) or biodegradation (Dawson et al., 2018) of larger items. Likewise, similarly to MP, primary NP from cosmetics (Hernandez et al., 2017), 3D-printing wastes (Stephens et al., 2013), lubricants (Dubey et al., 2015) or drugs (Lusher et al., 2017) are suspected to enter the oceans directly. The

increase of NP used in such industries – and thus their release in environment – is suspected although very little information is available regarding the actual quantities used and discarded. At sea, the presence of plastic particles lower than 1 µm has been recently argued in the Atlantic Gyre (Ter Halle et al., 2017). However, owing to a lack of methods, no or very little information is currently available about the environmental concentrations of NP and small MP particles (<100 µm), respectively (e.g. Huvet et al., 2016). Their environmental concentrations can only be estimated, for example following a power-law increase (around a 2.2 factor) from sea surface samples as recently proposed (Erni-Cassola et al., 2017).

Despite the lack of knowledge concerning MP and NP distributions in the oceans, a consensus exists about the threat posed by small plastic particles for aquatic life (GESAMP, 2015). Effects of MP on feeding behavior (Cole et al., 2013; Ogonowski et al., 2016), energy balance (Wright et al., 2013; Watts et al., 2015), reproduction (Sussarellu et al., 2016; Gardon et al., 2018), and immune system (Avio et al., 2015; Paul-Pont et al., 2016) were demonstrated and ecological impacts can be discerned (Rochman et al., 2015; Green et al., 2016; Galloway et al., 2017). Furthermore, at the nanoscale, specific effects are expected as result of the physico-chemical properties of NP (Mattsson et al. 2015a; da Costa et al., 2016). Nanoparticles have a much greater surface/volume ratio than microparticles – the number of surface atoms increases when size decreases – which enhances their reactivity in aquatic environments (Mattsson et al. 2015a, Rocha et al. 2015). Likewise, the risk of translocation and overall transfer into the tissues of organisms increases at the nanoscale. For instance, fluorescent nano-polystyrene beads (NP-PS; 50 nm) seemed dispersed in the body of *Paracyclopina nana* after ingestion, while MP (500 nm and 6 µm) remained in the digestive tract with a shorter retention time (Jeong et al., 2017). Initial assessments of NP toxicity highlighted risks to survival, feeding activity, embryogenesis, the

immune system, fecundity (number of offspring and/or pregnancy rate), metabolism (changes in amino acid composition, liver dysfunctions and energy balance) and behavior at a wide range of trophic levels including phytoplankton (Besseling et al., 2014), echinoderms (Della Torre et al., 2014), rotifers (Jeong et al., 2016), crustaceans (Cui et al., 2017; Jeong et al., 2017), bivalves (Wegner et al., 2012 ; Canesi et al., 2016) and fish (Mattsson et al. 2015b, Mattsson et al. 2017).

In the adult Pacific oyster *Crassostrea gigas* (Bayne et al., 2017), polystyrene microbeads of 2 and 6 µm were shown to interfere considerably with gametogenesis, in terms of quantity and quality of produced gametes, leading to undesirable effects on the performance of offspring despite no direct exposure (Sussarellu et al., 2016). Because *C. gigas* has external fertilization, the free-living stages (*i.e.* gametes, embryos and larvae) must cope with the stress occurring in estuarine and coastal marine habitats where oysters live. To date only one study has investigated the impacts of plastic debris exposure to Pacific oyster larvae using 1 and 10 µm MP with no effect on their growth rate or survival (Cole and Galloway, 2015). These authors also studied the ingestion of polystyrene particles spanning 70 nm to 20 µm in size, but no toxic endpoint was monitored following exposure to this size class. For gametes, carboxylic nanoplastics (100 nm) induced oxidative stress in oyster spermatozoa linked to an increase in ROS production (González-Fernández et al., 2018). In this context, the present study aims to assess the potential adverse effects of plastic items on Pacific oyster free-living stages, targeting specifically the essential steps of fertilization, embryo-larval development and metamorphosis, so as to provide a view over the complete life cycle in addition to the adult exposure of Sussarellu et al. (2016) (Fig. 1). Here, oyster gametes, embryos and larvae were exposed to five types of polystyrene particles, varying in size from NP to MP (50 nm; 500 nm; 2 µm) and in functionalization (no functional group, or presence of carboxyl or amine groups) to examine a size effect between MP and NP

104 (plain particles), as well as a surface properties effect between NP exhibiting different
105 functionalization. The behavior of the particles was measured in seawater using Dynamic Light
106 Scattering (DLS) to assess particle aggregation and modifications of the mean surface charge.

107 Materials and methods

108 Micro- and nanoplastic

109 Five commercially available polystyrene (PS) beads were purchased from Polysciences/Bangs
110 Laboratories and stored at 4°C prior to experiments: 50-nm, 500-nm and 2-µm beads without
111 functionalization (Plain), and 50-nm beads coated with carboxyl (COOH-50) or amine groups
112 (NH_2-50). Before each handling, particles were vortexed to prevent particle aggregation and
113 insure good suspension homogenization. Commercial suspensions were in ultrapure water (UW)
114 with Tween-20© surfactant (<0.1%) to limit aggregation; Tween-20© had previously been
115 demonstrated to be innocuous for marine invertebrates at this dose (Ostroumov, 2003). Raman
116 microspectroscopy analysis confirmed the PS nature of the polymer for all beads and no
117 additional features were observed in the PS spectra across all particles. (Fig. S1). All tests (DLS
118 and exposures) were performed with the same batch of particles.

119 Dynamic Light Scattering (DLS) analysis

120 DLS (Zetasizer NanoZS; Malvern Instruments; United Kingdom) was used to determine the
121 aggregation state (polydispersity index – PDI; Arbitrary Units (A.U.)), the mean size of
122 particles/aggregates (hydrodynamic diameter; nm) and the mean surface charge (ζ-potential; mV)
123 of MP/NP in two media: UW, as delivered by the supplier, and natural filtered seawater collected
124 from the Bay of Brest (FSW; 1-µm filtered and UV-treated; pH 8.1 and 34 PSU). When PDI
125 exceeds 0.2, particles were considered to be aggregated. Measurements were performed in

126 triplicate at 20°C (similar to the T°C used for bioassays) and a concentration of 100 µg/mL at T0
127 and T24h, each containing 13 runs (10 sec.measure^{-1}) for PDI and hydrodynamic diameter, and
128 40 runs (10 sec.measure^{-1}) for ζ-potential as conducted by González-Fernández et al. (2018). This
129 concentration was used for DLS analysis owing to the presence of artifacts at lower
130 concentrations.

131 **Suspensions of MP/NP for bioassays**

132 MP and NP stock suspensions were prepared in UW at 1,000 µg/mL, while working suspensions
133 were prepared in FSW. Four concentrations of plastic were tested: 0.1, 1, 10 and 25 µg/mL, plus
134 a control group (0 µg/mL), in order to identify toxicity thresholds. A total of 25 treatments (5
135 particle types × 5 concentrations) were then tested on the three early stages (gametes, embryos
136 and larvae; see below).

137 **Biological material**

138 Oysters from 2 cohorts, produced in 2014 and 2015 according to Petton et al. (2015), were
139 deployed in 2016 in the bay of Brest and in the Marennes-Oléron basin (France). In the summer
140 of 2017, oysters were randomly sampled to collect their gametes for assays on gametes and
141 embryo-larval development. For the metamorphosis assay, pediveliger larvae (21 days old) were
142 purchased from a commercial hatchery (Société Atlantique de Mariculture, France).

143 **Gamete assay**

144 Sperm from two males and oocytes from three females were collected by stripping the gonad.
145 This was repeated in five replicates, involving a total of 10 males and 15 females. Sperm were
146 then sieved at 100 µm, and oocytes at 100 µm then 20 µm to eliminate debris (Steele and
147 Mulcahy, 1999). Oocytes were diluted in 2 L and sperm in 100 mL of FSW maintained at 21°C ±

1°C (mean ± SD). Spermatozoa mobility and round shape of oocytes, used as proxies of gamete quality, were checked by microscopy (Olympus BX51; ×10-20 magnification with phase contrast for sperm) (Fabbri et al., 2014). Spermatozoa and oocyte concentrations were estimated by flow cytometry (EasyCyte Plus cytometer; Millipore Corporation; USA) (Le Goïc et al., 2014, 2013). Gametes (1,000 oocytes/mL; 100:1 spermatozoa:oocyte ratio) were placed at the same time in 40 mL glass vials filled with 30 mL of FSW at 21°C ± 1°C, containing the MP or NP suspensions (5 particle types × 5 concentrations; 5 replicates per treatment).

After 1.5 h, samples were fixed with a formaldehyde-seawater solution (0.1% final) to estimate the fertilization yield under a microscope (Zeiss Axio Observer Z1; ×10-40 magnification; observation of 150 oocytes per vial). The fertilization yield was defined as: (number of fertilized oocytes / [number of fertilized and unfertilized oocytes]) × 100 (Martínez-Gómez et al., 2017). An oocyte was considered to be fertilized when polar bodies and cell divisions were observed.

Embryo-larval assay

The standardized AFNOR procedure (AFNOR XP-T-90-382) was used to perform this assay. Fertilization was achieved in five replicates with gametes collected from five males and five females per replicate (total: 25 males and 25 females) following the procedure described above. Once fertilization was achieved in a 2-L glass beaker filled with 1.5 L of FSW with high fertilization yields (>90%; verified under a Zeiss Axio Observer Z1; ×10-40 magnification), 1,500 embryos were collected per replicate and diluted at a concentration of 60 embryos/mL in 40 mL glass vials filled with 25 mL of FSW (21°C ± 1°C) containing the MP or NP suspensions (5 particle types × 5 concentrations; 5 replicates per treatment). After 36 h in dark conditions, samples were fixed with a formaldehyde-seawater solution (0.1% final) to evaluate the D-larval

yield under a microscope (Zeiss Axio Observer Z1; ×10-63 magnification; observation of 100 larvae per vial). The D-larval yield was defined as: (number of normal D-larvae / number of normal and abnormal D-larvae) × 100 (Di Poi et al., 2014). A normal D-larvae indicated embryogenic success, while an abnormal larva presented mantle, shell and/or hinge malformations, or developmental arrest at the embryonic stage (Mottier et al., 2013).

Metamorphosis assay

The bioassay at the metamorphosis stage was performed as described in Di Poi et al. (2014). Briefly, a total of 65 ± 15 pediveliger larvae per treatment were exposed to plastic particles in 12-well microplates (NUNC© with the Nunclon™ Delta surface treatment) filled with 1.5 mL of FSW containing the MP or NP suspensions (5 particle types × 5 concentrations; 6 replicates per treatment) for 24 h at 21°C ± 1°C. Metamorphosis of oyster larvae was stimulated by adding 10^{-4} M epinephrine (Sigma-Aldrich; CAS number: 51-43-4) (Coon et al., 1990) immediately after the start of the exposure (Di Poi et al., 2014). After the 24 h incubation, samples were fixed with a formaldehyde-seawater solution (0.1% final) to determine the metamorphosis yield under a microscope (Leica DM-IRB; ×10 magnification; all larvae were observed). The metamorphosis yield was defined as: (number of metamorphosed larvae / total number of larvae) × 100. A metamorphosed larva is characterized by a significant growth of shell and gills, and loss of the velum and foot (Di Poi et al., 2014).

Statistical analyses

Statistical analyses and graphical representations were produced using the R software. Percentages were analyzed after angular transformation. Normality and homogeneity of variance were verified by the Shapiro-Wilk and Levene methods, respectively. The Student's *t*-test was

used to compare particle behavior (size and ζ-potential) between UW and FSW. For effects of particle concentrations on fertilization, embryo-larval development and metamorphosis success, parametric (ANOVA) or non-parametric (Kruskal-Wallis) analyses of variance were followed by post-hoc methods (Tukey or Conover) for pairwise comparisons when differences were detected. Whenever a dose-response pattern was observed, the package "DRC" was used to determine the half maximal effective concentration (EC_{50}), defined as the concentration of a substance leading to a significant effect in 50% of the population. All data are represented by means ± standard deviation (SD).

Results

Particle characterization

The 2-µm and 500-nm beads formed small aggregates in UW (PDI>0.2), whereas all NP remained in their original form (PDI<0.2; Table 1). For all particles, the aggregation state or size of aggregates increased significantly when added to seawater ($p<0.01$). Only the NH_2-50 formed aggregates at the nanometer scale (mean ± SD; 96.5 ± 2.0 nm) in FSW. The Plain-50 (5951.0 ± 264.3 nm) and COOH-50 (3735.0 ± 443.8 nm) formed larger aggregates than the 2-µm (3113.7 ± 32.3 nm) and 500-nm (1620.7 ± 188.8 nm) beads in FSW. All particles presented a negative surface charge in UW and FSW, with the exception of NH_2-50 that exhibited a positive surface charge in all media. The seawater systematically buffered the charge of all MP/NP with mean surface charge values decreasing towards zero in seawater compared to UW ($p<0.01$; Table 1). No significant changes ($p>0.05$) of charge and aggregation were observed between T0 and T24h in FSW for all particles except the Plain-50 which formed bigger aggregates exceeding 10 µm in FSW ($p<0.05$; Table S1).

Gamete assay

The control treatment (0 plastic) presented a high fertilization yield (mean ± SD; 92.3 ± 1.0%), demonstrating the good quality/maturity of the gametes and the quality of the FSW. The 2-µm (Fig. 2A) and 500-nm (Fig. 2B) particles had no effect on the fertilization yield relative to the control group ($p>0.05$). All NP significantly impaired the fertilization yield in a dose-response manner between 1 and 25 µg/mL. Exposure to Plain-50 (Fig. 2C) led to significant reductions in fertilization ($p<0.05$) of 2.7, 55.7 and 72.7% for 1, 10 and 25 µg/mL, respectively, associated with an EC_{50} value of 12.3 ± 7.5 µg/mL. The COOH-50 particles (Fig. 2D) induced significant decreases ($p<0.05$) of 3.8, 65.7 and 93.0% with an EC_{50} value of 7.8 ± 1.1 µg/mL. The NH_2-50 exhibited the strongest toxicity inducing significant decreases ($p<0.05$) in the fertilization yield of 6.3, 75.4 and 91.2% for increasing doses of NP associated with an EC_{50} value of 4.9 ± 0.9 µg/mL (Fig. 2E; Fig. S2).

Embryo-larval assay

Exposure to 2-µm (Fig. 3A) and 500-nm (Fig. 3B) did not cause any significant effect on embryo-larval development compared with the control treatment (mean ± SD; 93.3 ± 1.5%) at 36 hours post-fertilization (hfp). The D-larval yield was significantly reduced ($p<0.01$) by exposure to 10 and 25 µg/mL of Plain-50 (Fig. 3C) leading to a mean reduction of 9.2 and 16.9%, respectively. This was insufficient to estimate a robust EC_{50} value for the Plain-50 (Fig. S3). Exposure to COOH-50 led to a mean reduction of 32.2 and 100% after exposure to 10 and 25 µg/mL, respectively (Fig. 3D) with an EC_{50} value of 11.60 ± 10.5 µg/mL. The highest toxicity was observed for the NH_2-50 with a significant decrease of 6.4% ($p<0.05$) in the D-larval yield at the lowest concentration (0.1 µg/mL), followed by a total inhibition (100% reduction) of the

embryo-larval development success for higher doses giving an EC_{50} value of 0.15 ± 0.4 µg/mL (Fig. 3E; Fig. S3).

Compared to the control group where D-larvae appeared healthy (Fig. 4A), Plain-50 (10 and 25 µg/mL) and COOH-50 (10 µg/mL) caused numerous mantle or/and shell malformations (Fig. 4A-B). Only dead embryos/larvae were observed at the highest concentration of COOH-50 (Fig. 4D) whereas mainly cell debris were observed upon exposure to the three highest doses of NH_2-50 (Fig. 4E-F). In both cases, this represents evidence of developmental arrest.

Metamorphosis assay

A high metamorphosis yield was observed in all treatments, ranging from 81.5 ± 9.0 to 90.8 ± 2.4 (mean ± SD = 86.6 ± 3.6%), and no significant effect of MP/NP exposure ($p>0.05$) on metamorphosis success of *C. gigas* was demonstrated, regardless of particle type or concentration. Furthermore, no abnormalities were observed under a microscope for any of the treatments tested.

Discussion

Strong effects of NP were observed on the success of fertilization and embryogenesis of *C. gigas* depending on particle dose and functionalization. Based on the commercial size, a higher toxicity of NP compared to MP was demonstrated here, in agreement with previous observations across a range of species, including copepods (Jeong et al., 2017, 2016; Lee et al., 2013), crustaceans (Ma et al., 2016) and fish (Mattsson et al., 2017). This comparison was only done for plain particles, and the functionalization-dependent toxicity remains to be tested for MP, especially using amine groups displaying the strongest toxicity at the nanoscale. These insights support the purpose that risks of NP may be higher than microscale counterparts (Wright and Kelly, 2017). Indeed, there

258 is a consensus concerning the risk of nanomaterials as a result of their high reactivity and their
259 capacity to cross biological membranes (Nel et al., 2006). It is noteworthy that the short term
260 exposure to plain 500-nm and 2-µm beads did not show any effect on the two essential planktonic
261 stages of oyster reproduction and development (gametes and embryos), whereas deleterious
262 effects after 2-months of exposure to 2 and 6-µm plain PS beads were previously demonstrated
263 on gametogenesis of adult oysters leading to subsequent negative impacts on unexposed gametes
264 and offspring (Sussarellu et al., 2016).

265 The dose-response exposure experiments performed here, which are the recommended approach
266 when environmental concentrations are unknown (e.g. Paul-Pont et al., 2018), allowed the
267 estimation of the half maximal effective concentration (EC_{50}) indicating the concentration of a
268 compound when 50% of its maximal effect is observed. The lowest EC_{50} was observed for the
269 NH_2-50, which was 1.6 to 77 times more toxic for gametes and embryos, respectively, than the
270 COOH-50. The highest EC_{50} in NP exposures was observed for the Plain-50 particles presumably
271 due to a decrease of their bioavailability owing to the presence of aggregates higher than 10 µm
272 observed in seawater at T24h. Oyster embryos exhibited similar sensitivity as mussel embryos
273 (48h exposures; EC_{50} NH_2-50: 0.14 µg/mL)(Balbi et al., 2017), but their sensitivity was higher
274 than that of sea urchin embryos (48h exposures; EC_{50} NH_2-50: 2.61 µg/mL)(Della Torre et al.,
275 2014), suggesting inter-species variability. Additionally, biological stage within the same species
276 appears to be an important factor in determining effects, considering the absence of NP toxicity
277 on metamorphosis success. As demonstrated here, oyster larvae seem to withstand MP/NP
278 exposures, in agreement with a previous study showing no effect on growth rate or survival of
279 oyster larvae upon exposure to 1 and 10 µm PS particles for 8 days (Cole and Galloway, 2015).
280 The absence of toxicity of MP/NP on pediveliger oyster larvae is probably linked to a decrease in

the larvae surface/volume ratio, and/or the appearance of a shell protecting larvae from polystyrene particles (Hickman, 1999; Liebig and Vanderploeg, 1995; Schiaparelli et al., 2004).

The potential underlying mechanisms of NP toxicity include impairment of biological membranes, sub-cellular toxicity or physical blockages, notably for spermatozoa. These explanatory hypotheses, discussed below, are not mutually exclusive and could all play a role in the observed adverse effects of NH_2-50, Plain-50 and COOH-50 on oyster planktonic stages.

The observed toxicity of nano-PS on gametes and embryos may be related to damage caused by membrane breakages (Nel et al., 2009). Indeed, adhesion of nanoplastics on oyster gametes, both oocytes and spermatozoa (González-Fernández et al., 2018), and sea urchin and mussel embryos (Della Torre et al., 2014; Balbi et al., 2017) was recently demonstrated. We can rely on these published data from different models and particles to suggest that NP have stuck on oyster's gametes and embryos. Consequences might be significant for biological membranes: molecular simulations have demonstrated the capacity of nano-PS to perturb lipid membranes (Rossi et al., 2014). Even if metallic and plastic nanoparticles cannot be directly compared, nickel and iron nanoparticles reduced the membrane integrity of *Ciona instinalis* (Gallo et al., 2016) and *Mytilus edulis* spermatozoa, leading to a decrease in fertilization success (Kadar et al., 2011). Interactions between nanoparticles and biological membranes are driven by particle aggregation and size. Here, the most toxic nanoplastics (NH_2-50) remained at the nanometer size in seawater and were thus expected to interact more with biological membranes through their higher reactivity and capacity to cross biological membranes (Nel, 2006; Verma and Stellacci, 2010). Similarly, exposure to NH_2-50 led to higher toxicity in sea urchin embryos and shrimp larvae (Bergami et al., 2016; Della Torre et al., 2014), compared to COOH-40 nm forming approximatively 1 µm aggregates in seawater. The major differences in aggregation observed for the different

304 nanobeads in ultrapure water and filtered seawater are a result of the characteristics of the
305 nanobeads themselves and the surrounding medium (Nel et al., 2009; Rocha et al., 2015). The
306 high aggregation of COOH-50 and Plain-50 observed here in filtered seawater can be explained
307 by a strong interaction between the negative surface charge of these NP and the abundant cationic
308 ions such as Ca^{2+} in seawater. It is noteworthy that Plain-50 forming micrometric sized
309 aggregates led to significant toxicity on gametes and embryos while plain MP exhibiting lower
310 micrometric size (2µm) seemed innocuous. This suggests that nanoparticles remain highly
311 reactive with biological membrane even in the form of large aggregates.

312 The differential interactions between cells and nanoparticles may also be linked to their surface
313 properties, notably the net surface charge (Nel et al., 2009). The so-called buffering effect
314 observed on the net surface charge of MP/NP incubated in filtered seawater compared to
315 ultrapure water is also related to the presence of anions and cations in seawater that would have
316 interacted with their surface layer. The ions brought the ζ-Potential to a neutral surface charge,
317 and as a result, decreased NP stability (El Badawy et al., 2010; Lin et al., 2010). The lowest
318 surface charge observed for the Plain-50 may lead to reduced interaction with gamete and
319 embryo membranes, explaining their lower toxicity compared to other NP. Cationic nanoparticles
320 interact with negative membrane residuals more easily than anionic ones, and this interaction
321 triggers internalization to maintain the overall negative membrane charge, which may eventually
322 induce membrane disruptions (Cho et al., 2009; Fröhlich, 2012). Furthermore, a chemical effect
323 of the functionalization cannot be excluded and will be dependent on the commercial products
324 and their manufacturers.

325 Impairment of membrane integrity during cell divisions can lead to developmental arrest during
326 embryogenesis (Rossi et al., 2014), in agreement with the numerous malformations we observed

upon NP exposure. These results call for detailed microscopic analyses of exposed cell membranes, coupled with lipidomic approaches to assess lipid membrane composition upon NP exposure, in order to better understand the effects of NP on membrane integrity.

Given the high aggregation (3–10µm) observed in our data for the Plain-50 and COOH-50, congestion of gametes is a possibility; our previous study demonstrated the adhesion of carboxylic nanopolystyrene (100 nm) on oyster spermatozoa (González-Fernández et al., 2018). This congestion may hamper spermatozoa internalization into oocytes, leading to negative effects on the fertilization yield as observed upon exposure to Plain-50 and COOH-50.

Among the numerous physicochemical properties of the particles, including size, surface charge, aspect ratio, porosity that impact *in vivo* behavior of MP and NP, surface corona is of real importance (e.g. Galloway et al., 2017). Indeed, corona formation on nano-PS can fluctuate depending on the surface properties of the particle, *i.e.* functionalization and charge (Lundqvist et al., 2008). It can affect the particle chemical identity with significant consequences on ingestion and interaction with cells and organs (Hristov et al., 2015; Canesi et al., 2016; Nasser & Lynch, 2016). Further studies are required to characterize the NP-cell interactions (entry, adhesion and membrane impairments) in oyster gametes and embryos and to understand the toxic pathways involved.

At the same time, the NP toxicity observed here could be related to sub-cellular toxicity upon internalization and/or membrane disruption of gametes/embryos. For instance, NH_2-50 was better internalized in human cell lines representing various organs, and led to more cytotoxic effects than COOH-50 and Plain-50 (Anguissola et al., 2014; Bannunah et al., 2014). Similar mechanisms, involving NP entry leading to sub-cellular toxicity, could also be hypothesized here requiring fine microscopical observations using fluorescent NP. In the present study, the

exclusive occurrence of developmental arrest during exposure at the highest concentrations of NH_2-50 and COOH-50 could indicate the involvement of apoptosis pathways, as described in the sea urchin *Paracentrotus lividus* (Della Torre et al., 2014; Pinsino et al., 2017). The intermediate situation, where malformed larvae (mantle, shell and hinge malformations) were observed upon exposure to Plain-50, intermediate concentrations of COOH-50 and the lowest concentration of NH_2-50, could be a result of dysregulation of genes involved in shell mineralization, as previously demonstrated by transcriptional analysis in mussel embryos exposed to 0.15 µg/mL of NH_2-50. Another toxic effect, previously characterized during exposure to chemical agents and nanoplastics, involves a decrease in DNA integrity or a disruption of the cell oxidative balance of oyster gametes and embryos (Akcha et al., 2012; Behrens et al., 2016; Vignier et al., 2017; González-Fernández et al., 2018). Nanoparticles can interfere with electron transfer of the intracellular medium, inducing a production of ROS (superoxide anion / hydroxyl radical, hydrogen peroxide) and generating disruption of redox functions (Fu et al., 2014). This overproduction of ROS results in several types of damage, such as lipid peroxidation or DNA breakages leading to embryotoxicity (Xie et al., 2017). In agreement with these observations we previously suggested that spermatozoa may lose their ability to fertilize oocytes as a consequence of an oxidative stress induced by exposure of oyster spermatozoa to carboxylic nanopolystyrene (100 nm) (González-Fernández et al., 2018).

The lowest concentration (0.1 µg/mL) used here was five times higher than the mass concentration of MP used in the study of Sussarellu et al. (2016) based on equivalent mass concentration of >333µm plastics debris hotspots. At this concentration, only exposure of oyster embryos to NH_2-50 had a significant effect, which suggests that the probability of oyster planktonic stages suffering fertilization and embryo-larval development disruptions due to NP

exposure is low in nature at the present time. However, taking into account the calculations of Besseling et al. (2014), the toxic effects observed here began at lower concentrations than the highest mass concentration of plastic debris (16.9 µg/mL) estimated at the water-sediment interface. This location is known for its high plastic contamination and where wild adult oysters live and spawn (Martin et al., 2017). Furthermore, the power-law increase in MP concentration with decreasing particle size in sea surface samples suggests that small MP are increasingly abundant, and that MP concentrations will be underestimated if the smallest fraction is not properly quantified (Bergmann et al., 2017; Erni-Cassola et al., 2017).

With regards to the increase of (nano)plastics used in industry (GESAMP 2015), the recent estimation of their mismanagement and release into oceans worldwide, as well as the continuous breakdown of plastic waste at the nanometer scale, better management of end-of-life plastics is should be strongly recommend to enable a transition to a circular economy (Brink et al. 2017) and limit or prevent accidental releases. For instance, nano-TiO_2 levels are expected to reach up to 1 µg/mL in nature (Holden et al., 2014), although its estimated accidental release in the marine environment is much lower (between 2 and 6 million tons over the next 10 years (Haynes et al., 2017)) than that estimated for plastic wastes. The latter were estimated between 4.8 and 12.7 million tons in 2010 alone, with an expected increase of an order of magnitude by 2025 (Jambeck et al., 2015).

Conclusion

Our study is the first demonstration of adverse effects of nanoplastics on oyster early-life stages, with the fertilization/embryogenesis steps being particularly sensitive. The combination of fine microscopy and Omics (lipidomics, transcriptomics) tools is now needed to fully understand the underlying toxicity mechanisms that likely include both membrane disruption and sub-cellular

toxicity. Significant ecological implications can be expected as effects on gametes, fertilization and embryo-larval development determine recruitment, population stability and ecosystem structure. Indeed, oysters sustain the formation of reefs providing micro-habitats for a large community of invertebrates and nursery areas for pelagic organisms (Bayne, 2017). We suggest that direct effects on early-life stages should be integrated into the "adverse outcome pathway" (AOP) scheme describing microplastic toxicity pathways in aquatic organisms (Galloway and Lewis, 2016). Indeed, this additional pathway may influence the offspring viability and the overall reproductive output. In this context, our work highlights the interest of using oysters as a model to describe the risk of plastic debris in coastal and estuarine areas where a high spatial variability of contamination is expected.

Acknowledgment

This study was financially supported by the ANR-Nanoplastics project (ANR-15-CE34-0006). K. Tallec was funded by a French doctoral research grant from the region Bretagne (50%) and Ifremer (50%). The authors thank E. Fleury, M. Boulais, V. Foulon, J. Castrec, M. Suquet, A-L Cassone and the staff of the experimental station of Argenton, JL. Seugnet and the RESCO team for their help with the experimental work, PA. Jaffres and O. Lozach (UMR-CNRS 6521) for their support and expertise with the DLS, and H. McCombie for her help in editing the English.

References

Akcha, F., Spagnol, C., Rouxel, J., 2012. Genotoxicity of diuron and glyphosate in oyster spermatozoa and embryos. Aquat. Toxicol. 106–107, 104–113. https://doi.org/10.1016/j.aquatox.2011.10.018

Anguissola, S., Garry, D., Salvati, A., O'Brien, P.J., Dawson, K.A., 2014. High content analysis provides mechanistic insights on the pathways of toxicity induced by amine-modified polystyrene nanoparticles. PLoS One 9. https://doi.org/10.1371/journal.pone.0108025

Avio, C.G., Gorbi, S., Milan, M., Benedetti, M., Fattorini, D., D'Errico, G., Pauletto, M., Bargelloni, L., Regoli, F., 2015. Pollutants bioavailability and toxicological risk from microplastics to marine mussels. Environ. Pollut. 198, 211–222. https://doi.org/10.1016/j.envpol.2014.12.021

Balbi, T., Camisassi, G., Montagna, M., Fabbri, R., Franzellitti, S., Carbone, C., Dawson, K., Canesi, L., 2017. Impact of cationic polystyrene nanoparticles (PS-NH_2) on early embryo development of *Mytilus galloprovincialis*: Effects on shell formation. Chemosphere 186, 1–9. https://doi.org/10.1016/j.chemosphere.2017.07.120

Bannunah, A.M., Vllasaliu, D., Lord, J., Stolnik, S., 2014. Mechanisms of Nanoparticle Internalization and Transport Across an Intestinal Epithelial Cell Model: Effect of Size and Surface Charge. Mol. Pharm. 11, 4363–4373. https://doi.org/10.1021/mp500439c

Bayne, B., 2017. Biology of oyster 1st Edition. *Eds Academic Press*, 862 pp.

Bayne, B.L., Ahrens, M., Allen, S.K., D'auriac, M.A., Backeljau, T., Beninger, P., Bohn, R., Boudry, P., Davis, J., Green, T., Guo, X., Hedgecock, D., Ibarra, A., Kingsley-Smith, P., Krause, M., Langdon, C., Lapègue, S., Li, C., Manahan, D., Mann, R., Perez-Paralle, L., Powell, E.N., Rawson, P.D., Speiser, D., Sanchez, J.-L., Shumway, S., Wang, H., 2017. The Proposed Dropping of the Genus Crassostrea for All Pacific Cupped Oysters and Its Replacement by a New Genus Magallana: A Dissenting View. J. Shellfish Res. 36, 545–547. https://doi.org/10.2983/035.036.0301

Behrens, D., Rouxel, J., Burgeot, T., Akcha, F., 2016. Comparative embryotoxicity and genotoxicity of the herbicide diuron and its metabolites in early life stages of *Crassostrea gigas*: Implication of reactive oxygen species production. Aquat. Toxicol. 175, 249–259. https://doi.org/10.1016/j.aquatox.2016.04.003

Bergami, E., Bocci, E., Luisa, M., Monopoli, M., Salvati, A., Dawson, K.A., Corsi, I., 2016. Nano-sized polystyrene affects feeding, behavior and physiology of brine shrimp *Artemia franciscana* larvae. Ecotoxicol. Environ. Saf. 123, 18–25. https://doi.org/10.1016/j.ecoenv.2015.09.021

Bergmann, M., Wirzberger, V., Krumpen, T., Lorenz, C., Primpke, S., Tekman, M.B., Gerdts, G., 2017. High quantities of microplastic in Arctic deep-sea sediments from the HAUSGARTEN observatory. Environ. Sci. Technol. acs.est.7b03331. https://doi.org/10.1021/acs.est.7b03331

Besseling, E., Wang, B., Lürling, M., Koelmans, A.A., 2014. Nanoplastic affects growth of S. obliquus and reproduction of D. magna. Environ. Sci. Technol. 48, 12336–12343. https://doi.org/10.1021/es503001d

Canesi, L., Ciacci, C., Fabbri, R., Balbi, T., Salis, A., Damonte, G., Cortese, K., Caratto, V., Monopoli, M.P., Dawson, K., Bergami, E., Corsi, I., 2016. Interactions of cationic polystyrene nanoparticles with marine bivalve hemocytes in a physiological environment: Role of soluble hemolymph proteins. Environ. Res. 150, 73–81. https://doi.org/10.1016/j.envres.2016.05.045

Cho, E.C., Xie, J., Wurm, P.A., Xia, Y., 2009. Understanding the role of surface charges in cellular adsorption versus internalization by selectively removing gold nanoparticles on the cell surface with a I 2/KI etchant. Nano Lett. 9, 1080–1084. https://doi.org/10.1021/nl803487r

Cole, M., Galloway, T.S., 2015. Ingestion of Nanoplastics and Microplastics by Pacific Oyster Larvae. Environ. Sci. Technol. 49, 14625–14632. https://doi.org/10.1021/acs.est.5b04099

Cole, M., Lindeque, P., Fileman, E., Halsband, C., Goodhead, R., Moger, J., Galloway, T.S., 2013. Microplastic ingestion by zooplankton. Environ. Sci. Technol. 47, 6646–6655. https://doi.org/10.1021/es400663f

Cole, M., Lindeque, P., Halsband, C., Galloway, T.S., 2011. Microplastics as contaminants in the marine environment : A review. Mar. Pollut. Bull. 62, 2588-2597. https://doi.org/10.1016/j.marpolbul.2011.09.025

Coon, S.L., Walch, M., Fitt, W.K., Weiner, R.M., Bonar, D.B., 1990. Ammonia Induces Settlement Behavior in Oyster Larvae. Biol. Bull. 179, 297–303. https://doi.org/10.2307/1542321

Cózar, A., Martí, E., Duarte, C.M., García-de-Lomas, J., van Sebille, E., Ballatore, T.J., Eguíluz, V.M., González-Gordillo, J.I., Pedrotti, M.L., Echevarría, F., Troublè, R., Irigoien, X., 2017. The Arctic Ocean as a dead end for floating plastics in the North Atlantic branch of the Thermohaline Circulation. Sci. Adv. 3, e1600582. https://doi.org/10.1126/sciadv.1600582

Cui, R., Kim, S.W., An, Y.-J., 2017. Polystyrene nanoplastics inhibit reproduction and induce abnormal embryonic development in the freshwater crustacean *Daphnia galeata*. Sci. Rep. 7, 12095. https://doi.org/10.1038/s41598-017-12299-2

da Costa, J.P., Santos, P.S.M., Duarte, A.C., Rocha-Santos, T., 2016. (Nano)plastics in the environment - Sources, fates and effects. Sci. Total Environ. 566–567, 15–26. https://doi.org/10.1016/j.scitotenv.2016.05.041

Dawson, A.L., Kawaguchi, S., King, C.K., Townsend, K.A., King, R., Huston, W.M., Bengtson Nash, S.M., 2018. Turning microplastics into nanoplastics through digestive fragmentation by Antarctic krill. Nat. Commun. 9, 1001. https://doi.org/10.1038/s41467-018-03465-9

Della Torre, C., Bergami, E., Salvati, A., Faleri, C., Cirino, P., Dawson, K.A., Corsi, I., 2014. Accumulation and Embryotoxicity of Polystyrene Nanoparticles at Early Stage of Development of Sea Urchin Embryos *Paracentrotus lividus*. Environ. Sci. Technol. 48, 12302–12311. https://doi.org/10.1021/es502569w

Di Poi, C., Evariste, L., Serpentini, A., Halm-Lemeille, M.P., Lebel, J.M., Costil, K., 2014. Toxicity of five antidepressant drugs on embryo–larval development and metamorphosis success in the Pacific oyster, *Crassostrea gigas*. Environ. Sci. Pollut. Res. 21, 13302–13314. https://doi.org/10.1007/s11356-013-2211-y

Dubey, M.K., Bijwe, J., Ramakumar, S.S. V, 2015. Nano-PTFE: New entrant as a very promising EP additive. Tribol. Int. 87, 121–131. https://doi.org/10.1016/j.triboint.2015.01.026

El Badawy, A.M., Luxton, T.P., Silva, R.G., Scheckel, K.G., Suidan, M.T., Tolaymat, T.M., 2010. Impact of Environmental Conditions (pH, Ionic Strength, and Electrolyte Type) on the Surface Charge and Aggregation of Silver Nanoparticles Suspensions. Environ. Sci. Technol. 44, 1260–1266. https://doi.org/10.1021/es902240k

Eriksen, M., Lebreton, L.C.M., Carson, H.S., Thiel, M., Moore, C.J., Borerro, J.C., Galgani, F., Ryan, P.G., Reisser, J., 2014. Plastic Pollution in the World's Oceans: More than 5 Trillion Plastic Pieces Weighing over 250,000 Tons Afloat at Sea. PLoS One 9, 1–15. https://doi.org/10.1371/journal.pone.0111913

Erni-Cassola, G., Gibson, M.I., Thompson, R.C., Christie-Oleza, J.A., 2017. Lost, but Found with Nile Red: A Novel Method for Detecting and Quantifying Small Microplastics (1 mm to 20 μm) in Environmental Samples. Environ. Sci. Technol. 51, 13641–13648. https://doi.org/10.1021/acs.est.7b04512

Fabbri, R., Montagna, M., Balbi, T., Raffo, E., Palumbo, F., Canesi, L., 2014. Adaptation of the bivalve embryotoxicity assay for the high throughput screening of emerging contaminants in *Mytilus galloprovincialis*. Mar. Environ. Res. 99, 1–8. https://doi.org/10.1016/j.marenvres.2014.05.007

Fröhlich, E., 2012. The role of surface charge in cellular uptake and cytotoxicity of medical nanoparticles. Int. J. Nanomedicine 7, 5577. https://doi.org/10.2147/IJN.S36111

Fu, P.P., Xia, Q., Hwang, H.-M., Ray, P.C., Yu, H., 2014. Mechanisms of nanotoxicity: generation of reactive oxygen species. J. food drug Anal. 22, 64–75. https://doi.org/10.1016/j.jfda.2014.01.005

Gallo, A., Boni, R., Buttino, I., Tosti, E., 2016. Spermiotoxicity of nickel nanoparticles in the marine invertebrate *Ciona intestinalis* (ascidians). Nanotoxicology 10, 1096–1104. https://doi.org/10.1080/17435390.2016.1177743

Galloway, T.S., Cole, M., Lewis, C., Atkinson, A., Allen, J.I., 2017. Interactions of microplastic debris throughout the marine ecosystem. Nat. Ecol. Evol. 1, 116. https://doi.org/10.1038/s41559-017-0116

Galloway, T.S., Lewis, C.N., 2016. Marine microplastics spell big problems for future generations. Proc. Natl. Acad. Sci. USA 113, 2331–2333. https://doi.org/10.1073/pnas.1600715113

Gardon, T., Reisser, C., Soyez, C., Quillien, V., & Le Moullac, G., 2018. Microplastics Affect Energy Balance and Gametogenesis in the Pearl Oyster *Pinctada margaritifera*. Environmental Science & technology, 52(9), 5277-5286.

GESAMP (2015). "Sources, fate and effects of microplastics in the marine environment: a global assessment" (Kershaw, P. J., ed.). (IMO/FAO/UNESCO-IOC/UNIDO/WMO/IAEA/UN/UNEP/UNDP Joint Group of Experts on the Scientific Aspects of Marine Environmental Protection). Rep. Stud. GESAMP No. 90, 96.

Geyer, R., Jambeck, J.R., Law, K.L., 2017. Production, use, and fate of all plastics ever made. Sci. Adv. 3, e1700782. https://doi.org/10.1126/sciadv.1700782

Gigault, J., Ter Halle, A., Baudrimont, M., Pascal, P., Gauffre, F., Phi, T.-L., El Hadri, H., Grassl, B., Reynaud, S., 2018. Current opinion: What is a nanoplastic? Environ. Pollut. 235, 1030–1034. https://doi.org/10.1016/j.envpol.2018.01.024

Gigault, J., Pedrono, B., Maxit, B., Ter Halle, A., 2016. Marine plastic litter: the unanalyzed nano-fraction. Environ. Sci. Nano 3, 346–350. https://doi.org/10.1039/C6EN00008H

González-Fernández, C., Tallec, K., Le Goïc, N., Lambert, C., Soudant, P., Huvet, A., Suquet, M., Berchel, M., Paul-Pont, I., 2018. Cellular responses of Pacific oyster (*Crassostrea gigas*) gametes exposed in vitro to polystyrene nanoparticles. Chemosphere 208, 764–772. https://doi.org/10.1016/j.chemosphere.2018.06.039

Green, D.S., Boots, B., O'Connor, N.E., Thompson, R., 2016. Microplastics affect the ecological functioning of an important biogenic habitat. Environ. Sci. Technol. 51, 68–77. https://doi.org/10.1021/acs.est.6b04496

Haynes, V.N., Ward, J.E., Russell, B.J., Agrios, A.G., 2017. Photocatalytic effects of titanium dioxide nanoparticles on aquatic organisms—Current knowledge and suggestions for future research. Aquat. Toxicol. 185, 138–148. https://doi.org/10.1016/j.aquatox.2017.02.012

Hernandez, L.M., Yousefi, N., Tufenkji, N., 2017. Are There Nanoplastics in Your Personal Care Products? Environ. Sci. Technol. Lett. 4, 280–285. https://doi.org/10.1021/acs.estlett.7b00187

554 Hickman, C.S., 1999. Adaptive Function of Gastropod Larval Shell Features. Invertebr. Biol.
555 118, 346–356. https://doi.org/ 10.2307/3227006

556 Holden, P.A., Klaessig, F., Turco, R.F., Priester, J.H., Rico, C.M., Avila-Arias, H., Mortimer, M.,
557 Pacpaco, K., Gardea-Torresdey, J.L., 2014. Evaluation of Exposure Concentrations Used in
558 Assessing Manufactured Nanomaterial Environmental Hazards: Are They Relevant?
559 Environ. Sci. Technol. 48, 10541–10551. https://doi.org/10.1021/es502440s

560 Hristov, D.R., Rocks, L., Kelly, P.M., Thomas, S.S., Pitek, A.S., Verderio, P., Mahon, E.,
561 Dawson, K.A., (2015). Tuning of nanoparticle biological functionality through controlled
562 surface chemistry and characterisation at the bioconjugated nanoparticle surface. Sci. Rep, 5,
563 17040. https://doi.org/10.1038/srep17040.

564 Huvet, A., Paul-Pont, I., Fabioux, C., Lambert, C., Suquet, M., Thomas, Y., Robbens, J.,
565 Soudant, P., Sussarellu, R., 2016. Reply to Lenz et al.: Quantifying the smallest
566 microplastics is the challenge for a comprehensive view of their environmental impacts.
567 Proc. Natl. Acad. Sci. USA 113, E4123–E4124. https://doi.org/10.1073/pnas.1607221113

568 Jambeck, J.R., Geyer, R., Wilcox, C., Siegler, T.R., Perryman, M., Andrady, A., Narayan, R.,
569 Law, K.L., 2015. Plastic waste inputs from land into the ocean. Science 347, 768–771.
570 https://doi.org/10.1126/science.1260352

571 Jeong, C.B., Kang, H.M., Lee, M.C., Kim, D.H., Han, J., Hwang, D.S., Souissi, S., Lee, S.J.,
572 Shin, K.H., Park, H.G., Lee, J.S., 2017. Adverse effects of microplastics and oxidative
573 stress-induced MAPK/Nrf2 pathway-mediated defense mechanisms in the marine copepod
574 *Paracyclopina nana*. Sci. Rep. 7, 1–11. https://doi.org/10.1038/srep41323

575 Jeong, C.B., Won, E.J., Kang, H.M., Lee, M.C., Hwang, D.S., Hwang, U.K., Zhou, B., Souissi,
576 S., Lee, S.J., Lee, J.S., 2016. Microplastic Size-Dependent Toxicity, Oxidative Stress
577 Induction, and p-JNK and p-p38 Activation in the Monogonont Rotifer (*Brachionus*
578 *koreanus*). Environ. Sci. Technol. 50, 8849–8857. https://doi.org/10.1021/acs.est.6b01441

579 Kadar, E., Tarran, G.A., Jha, A.N., Al-Subiai, S.N., 2011. Stabilization of engineered zero-valent
580 nanoiron with Na-acrylic copolymer enhances spermiotoxicity. Environ. Sci. Technol. 45,
581 3245–3251. https://doi.org/10.1021/es1029848

582 Klaine, S.J., Koelmans, A.A., Horne, N., Carley, S., Handy, R.D., Kapustka, L., Nowack, B., von
583 der Kammer, F., 2012. Paradigms to assess the environmental impact of manufactured
584 nanomaterials. Environ. Toxicol. Chem. 31, 3–14. https://doi.org/10.1002/etc.733

585 Lambert, S., Wagner, M., 2016. Characterisation of nanoplastics during the degradation of
586 polystyrene. Chemosphere 145, 265–268.
587 https://doi.org/10.1016/j.chemosphere.2015.11.078

588 Lavers, J.L., Bond, A.L., 2017. Exceptional and rapid accumulation of anthropogenic debris on
589 one of the world's most remote and pristine islands. Proc. Natl. Acad. Sci. USA 114, 6052–
590 6055. https://doi.org/10.1073/pnas.1619818114

591 Le Goïc, N., Hégaret, H., Boulais, M., Béguel, J.-P., Lambert, C., Fabioux, C., Soudant, P., 2014.
592 Flow cytometric assessment of morphology, viability, and production of reactive oxygen
593 species of *Crassostrea gigas* oocytes. Application to Toxic dinoflagellate (*Alexandrium*
594 *minutum*) exposure. Cytom. Part A 85, 1049–1056. https://doi.org/10.1002/cyto.a.22577

595 Le Goïc, N., Hégaret, H., Fabioux, C., Miner, P., Suquet, M., Lambert, C., Soudant, P., 2013.
596 Impact of the toxic dinoflagellate *Alexandrium catenella* on Pacific oyster reproductive
597 output: application of flow cytometry assays on spermatozoa. Aquat. Living Resour. 26,
598 221–228. https://doi.org/10.1051/alr/2013047

599 Lee, K., Shim, W.J., Kwon, O.Y., Kang, J., 2013. Size-Dependent Effects of Micro Polystyrene
600 Particles in the Marine Copepod *Tigriopus japonicus*. Environ. Sci. Technol. 47, 11278–
601 11283. https://doi.org/dx.doi.org/10.1021/es401932b

602 Liebig, J.R., Vanderploeg, H.A., 1995. Vulnerability of *Dreissena polymorpha* Larvae to
603 Predation by Great Lakes Calanoid Copepods: the Importance of the Bivalve Shell. J. Great
604 Lakes Res. 21, 353–358. https://doi.org/10.1016/S0380-1330(95)71046-2

605 Lin, D., Tian, X., Wu, F., Xing, B., 2010. Fate and Transport of Engineered Nanomaterials in the
606 Environment. J. Environ. Qual. 39, 1896. https://doi.org/10.2134/jeq2009.0423

607 Lundqvist, M., Stigler, J., Elia, G., Lynch, I., Cedervall, T., Dawson, K.A, 2008. Nanoparticle
608 size and surface properties determine the protein corona with possible implications for
609 biological impacts. Proc. Natl. Acad. Sci. USA 105, 14265–14270.
610 https://doi.org/10.1073/pnas.0805135105

611 Lusher, A. L., Hollman, P. C. H., Mendoza-Hill, J. J., 2017. Microplastics in Fisheries and
612 Aquaculture: Status of Knowledge on their Occurrence and Implications for Aquatic
613 Organisms and Food Safety. FAO Fisheries and Aquaculture Technical Paper. No. 615, 147
614 pp.

615 Ma, Y., Huang, A., Cao, S., Sun, F., Wang, L., Guo, H., Ji, R., 2016. Effects of nanoplastics and
616 microplastics on toxicity, bioaccumulation, and environmental fate of phenanthrene in fresh
617 water. Environ. Pollut. 219, 166–173. https://doi.org/10.1016/j.envpol.2016.10.061

618 Martin, J., Lusher, A., Thompson, R.C., Morley, A., 2017. The Deposition and Accumulation of
619 Microplastics in Marine Sediments and Bottom Water from the Irish Continental Shelf. Sci.
620 Rep. 1–9. https://doi.org/10.1038/s41598-017-11079-2

621 Martínez-Gómez, C., León, V.M., Calles, S., Gomáriz-Olcina, M., Vethaak, A.D., 2017. The
622 adverse effects of virgin microplastics on the fertilization and larval development of sea
623 urchins. Mar. Environ. Res. 130, 69–76. https://doi.org/10.1016/j.marenvres.2017.06.016

624 Mattsson, K., Hansson, L.-A., Cedervall, T., 2015a. Nano-plastics in the aquatic environment.
625 Environ. Sci. Process. Impacts 17, 1712–1721. https://doi.org/10.1039/C5EM00227C

626 Mattsson, K., Ekvall, M.T., Hansson, L.A., Linse, S., Malmendal, A., Cedervall, T., 2015b.
627 Altered behavior, physiology, and metabolism in fish exposed to polystyrene nanoparticles.
628 Environ. Sci. Technol. 49, 553–561. https://doi.org/10.1021/es5053655

629 Mattsson, K., Johnson, E. V., Malmendal, A., Linse, S., Hansson, L.-A., Cedervall, T., 2017.
630 Brain damage and behavioural disorders in fish induced by plastic nanoparticles delivered
631 through the food chain. Sci. Rep. 7, 11452. https://doi.org/10.1038/s41598-017-10813-0

632 Mottier, A., Kientz-Bouchart, V., Serpentini, A., Lebel, J.M., Jha, A.N., Costil, K., 2013. Effects
633 of glyphosate-based herbicides on embryo-larval development and metamorphosis in the
634 Pacific oyster, *Crassostrea gigas*. Aquat. Toxicol. 128–129, 67–78.
635 https://doi.org/10.1016/j.aquatox.2012.12.002

636 Nasser, F., Lynch, I., 2016. Secreted protein eco-corona mediates uptake and impacts of
637 polystyrene nanoparticles on *Daphnia magna*. J. Proteomics 137, 45-51.
638 https://doi.org/10.1016/j.jprot.2015.09.005

639 Nel, A., Xia, T., Mädler, L., Li, N., 2006. Toxic Potential of Materials at the Nanolevel. Science.
640 311, 622–627. https://doi.org/10.1126/science.1114397

641 Nel, A.E., Mädler, L., Velegol, D., Xia, T., Hoek, E.M. V, Somasundaran, P., Klaessig, F.,
642 Castranova, V., Thompson, M., 2009. Understanding biophysicochemical interactions at the
643 nano-bio interface. Nat. Mater. 8, 543–557. https://doi.org/10.1038/nmat2442

644 Ogonowski, M., Schür, C., Jarsén, Å., Gorokhova, E., 2016. The Effects of Natural and
645 Anthropogenic Microparticles on Individual Fitness in *Daphnia magna*. PLoS One 11,
646 e0155063. https://doi.org/10.1371/journal.pone.0155063

647 Ostroumov, S.A., 2003. Studying effects of some surfactants and detergents on filter-feeding
648 bivalves. Hydrobiologia 500, 341–344. https://doi.org/10.1023/A:1024604904065

649 Paul-Pont, I., Tallec, K., González Fernández, C., Lambert, C., Vincent, D., Mazurais, D.,
650 Zambonino-Infante, J-L., Brotons, G., Lagarde, F., Fabioux, F., Soudant, P., Huvet, A.,
651 2018. Constraints and Priorities for Conducting Experimental Exposures of Marine
652 Organisms to Microplastics. Front. Mar. Sci. 5, 252.
653 https://doi.org/10.3389/fmars.2018.00252

654 Paul-Pont, I., Lacroix, C., González Fernández, C., Hégaret, H., Lambert, C., Le Goïc, N., Frère,
655 L., Cassone, A.-L., Sussarellu, R., Fabioux, C., Guyomarch, J., Albentosa, M., Huvet, A.,
656 Soudant, P., 2016. Exposure of marine mussels *Mytilus* spp. to polystyrene microplastics:
657 Toxicity and influence on fluoranthene bioaccumulation. Environ. Pollut. 216, 724-737.
658 https://doi.org/10.1016/j.envpol.2016.06.039

659 Petton, B., Boudry, P., Alunno-Bruscia, M., Pernet, F., 2015. Factors influencing disease-induced
660 mortality of Pacific oysters *Crassostrea gigas*. Aquac. Environ. Interact. 6, 205–222.
661 https://doi.org/10.3354/aei00125

662 Pinsino, A., Bergami, E., Della Torre, C., Vannuccini, M.L., Addis, P., Secci, M., Dawson, K.A.,
663 Matranga, V., Corsi, I., 2017. Amino-modified polystyrene nanoparticles affect signalling
664 pathways of the sea urchin (*Paracentrotus lividus*) embryos. Nanotoxicology 11, 201–209.
665 https://doi.org/10.1080/17435390.2017.1279360

666 Rocha, T.L., Gomes, T., Sousa, V.S., Mestre, N.C., Bebianno, M.J., 2015. Ecotoxicological
667 impact of engineered nanomaterials in bivalve molluscs: An overview. Mar. Environ. Res.
668 111, 74–88. https://doi.org/10.1016/j.marenvres.2015.06.013

669 Rochman, C.M., Browne, M.A., Underwood, A.J., van Franeker, J.A., Thompson, R.C., Amaral-
670 Zettler, L.A., 2015. The ecological impacts of marine debris: unraveling the demonstrated
671 evidence from what is perceived. Ecology 96, 301–312. https://doi.org/10.1890/14-2070.1

672 Rossi, G., Barnoud, J., Monticelli, L., 2014. Polystyrene nanoparticles perturb lipid membranes.
673 J. Phys. Chem. Lett. 5, 241–246. https://doi.org/10.1021/jz402234c

674 Schiaparelli, S., Cattaneo-Vietti, R., Mierzejewski, P., 2004. A “protective shell” around the
675 larval cocoon of *Cephalodiscus densus* Andersson, 1907 (Graptolithoidea, Hemichordata).
676 Polar Biol. 27, 813–817. https://doi.org/10.1007/s00300-004-0661-x

677 Steele, S., Mulcahy, M.F.O., 1999. Gametogenesis of the oyster *Crassostrea gigas* in southern
678 Ireland. J. Mar. Biol. Assoc. UK. 79, 673–686.

679 Stephens, B., Azimi, P., El Orch, Z., Ramos, T., 2013. Ultrafine particle emissions from desktop
680 3D printers. Atmos. Environ. 79, 334–339. https://doi.org/10.1016/j.atmosenv.2013.06.050

681 Sussarellu, R., Suquet, M., Thomas, Y., Lambert, C., Fabioux, C., Pernet, M.E.J., Le Goïc, N.,
682 Quillien, V., Mingant, C., Epelboin, Y., Corporeau, C., Guyomarch, J., Robbens, J., Paul-
683 Pont, I., Soudant, P., Huvet, A., 2016. Oyster reproduction is affected by exposure to
684 polystyrene microplastics. Proc. Natl. Acad. Sci. USA 201519019.
685 https://doi.org/10.1073/pnas.1519019113

686 ten Brink, P., Schweitzer J-P., Watkins, E., De Smet, M., Leslie, H., Galgani, F., 2017. T20 Task

687 Force Circular Economy Circular Economy Measures to Keep Plastics and Their Value in
688 the Economy. G20 Insights, 1–12.

689 Ter Halle, A., Jeanneau, L., Martignac, M., Jardé, E., Pedrono, B., Brach, L., Gigault, J., 2017.
690 Nanoplastic in the North Atlantic Subtropical Gyre. Environ. Sci. Technol. 51, 13689–
691 13697. https://doi.org/10.1021/acs.est.7b03667

692 Van Cauwenberghe, L., Devriese, L., Galgani, F., Robbens, J., Janssen, C.R., 2015. Microplastics
693 in sediments: A review of techniques, occurrence and effects. Mar. Environ. Res. 111, 5–17.
694 https://doi.org/10.1016/j.marenvres.2015.06.007

695 Verma, A., Stellacci, F., 2010. Effect of surface properties on nanoparticle-cell interactions.
696 Small 6, 12–21. https://doi.org/10.1002/smll.200901158

697 Vignier, J., Volety, A.K., Rolton, A., Le Goïc, N., Chu, F.L.E., Robert, R., Soudant, P., 2017.
698 Sensitivity of eastern oyster (*Crassostrea virginica*) spermatozoa and oocytes to dispersed
699 oil: Cellular responses and impacts on fertilization and embryogenesis. Environ. Pollut. 225,
700 270–282. https://doi.org/10.1016/j.envpol.2016.11.052

701 Vogeler, S., Bean, T. P., Lyons, B. P., Galloway, T. S. (2016). Dynamics of nuclear receptor gene
702 expression during Pacific oyster development. BMC Dev. Biol, 16, 33.
703 https://doi.org/10.1186/s12861-016-0129-6

704 Watts, A.J.R., Urbina, M.A., Corr, S., Lewis, C., Galloway, T.S., 2015. Ingestion of Plastic
705 Microfibers by the Crab *Carcinus maenas* and Its Effect on Food Consumption and Energy
706 Balance. Environ. Sci. Technol. 49, 14597–14604. https://doi.org/10.1021/acs.est.5b04026

707 Wegner, A., Besseling, E., Foekema, E.M., Kamermans, P., Koelmans, A.A., 2012. Effects of
708 nanopolystyrene on the feeding behavior of the blue mussel (*Mytilus edulis* L.). Environ.
709 Toxicol. Chem. 31, 2490–2497. https://doi.org/10.1002/etc.1984

710 Wright, S.L., Kelly, F.J., 2017. Plastic and Human Health: A Micro Issue? Environ. Sci. Technol.
711 51, 6634–6647. https://doi.org/10.1021/acs.est.7b00423

712 Wright, S.L., Rowe, D., Thompson, R.C., Galloway, T.S., 2013. Microplastic ingestion decreases
713 energy reserves in marine worms. Curr. Biol. 23, R1031–R1033.
714 https://doi.org/10.1016/j.cub.2013.10.068

715 Xie, J., Yang, D., Sun, X., Cao, R., Chen, L., Wang, Q., Li, F., Wu, H., Ji, C., Cong, M., Zhao, J.,
716 2017. Individual and Combined Toxicities of Benzo[a]pyrene and 2,2″,4,4″-
717 Tetrabromodiphenyl Ether on Early Life Stages of the Pacific Oyster, *Crassostrea gigas*.
718 Bull. Environ. Contam. Toxicol. 99, 582–588. https://doi.org/10.1007/s00128-017-2164-9

719

720 **Table legend**

721 **Table 1.** Mean size (in nm), aggregation state (PDI in arbitrary units, A.U.) and charge (ζ-
722 Potential in mV) of polystyrene particles in ultrapure water (UW), and UV-treated 1-µm filtered
723 seawater (FSW). Analyses were performed by Dynamic Light Scattering (DLS) at 20°C in
724 triplicate and data are represented as means ± SD. Comparisons were made between media using
725 the Student's t-test; * : $p<0.05$, ** $p<0.01$, *** $p<0.001$.

726 **Figure legends**

727 **Fig. 1** Life cycle of oyster showing the results of exposures on different stages to MP/NP. This
728 scheme was modified from Vogeler et al. (2016).

729 **Fig. 2** Fertilization yield (%) after 1.5 h exposure of oyster gametes (1,000 oocytes.mL^{-1}; 100:1
730 spermatozoa:oocyte ratio) to (A) 2-µm, (B) 500-nm, (C) Plain-50 nm, (D) COOH-50 nm, (E)
731 NH_2-50 nm polystyrene beads at five concentrations: 0, 0.1, 1, 10 and 25 µg/mL. The assay was
732 replicated five times and data are represented as means ± SD. Multiple comparisons were made
733 between treatments using Tukey's HSD (500-nm, NH_2-50) or Conover (Plain-50, COOH-50)
734 methods at the 5% alpha level; homogeneous groups are indicated by the same letter.

735 **Fig. 3** D-larval yield (%) after 36 h exposure of fertilized eggs to (A) 2-µm, (B) 500-nm, (C)
736 Plain-50 nm, (D) COOH-50 nm, (E) NH_2-50 nm polystyrene beads at five concentrations: 0, 0.1,
737 1, 10 and 25 µg/mL. The assay was replicated five times and data are represented as mean ± SD.
738 Multiple comparisons were made between treatments using Tukey's HSD (Plain-50, COOH-50)
739 or Conover (NH_2-50) methods at the 5% alpha level; homogeneous groups are indicated by the
740 same letter.

741 **Fig. 4** Microscopy panel of embryo-larval development success after 36 h exposure to
742 polystyrene nanobeads compared with normal D-larvae observed in the control treatment (A),
743 larvae with shell and/or mantle malformations after exposure to Plain-50 (25 µg/mL) (B), and
744 COOH-50 (10 µg/mL) (C). Only developmental arrest, dead larvae and cell debris were observed
745 for all embryos following exposure to 25 µg/mL of COOH-50 (D) and from 1 to 25 µg/mL of
746 NH_2-50 (E and F). Size in µm is represented by the scale bar.

747 **Table 1**

Media	Particles	Commercial Size (nm)	Particle/Aggregate Size (nm)	PDI (A.U.)	ζ-Potential (mV)
UW	2-µm	2,000	2681.0 ± 50.5	0.35 ± 0.01	-44.8 ± 0.9
	500-nm	500	774.3 ± 29.3	0.46 ± 0.05	-67.8 ± 7.0
	COOH-50	50	55.9 ± 0.4	0.06 ± 0.01	-62.1 ± 0.4
	Plain-50	50	49 ± 0.4	0.03 ± 0.02	-70.1 ± 1.4
	NH_2-50	50	53.3 ± 2.3	0.12 ± 0.02	44.0 ± 1.5
FSW	2-µm	2,000	3113.7 ± 32.3***	0.42 ± 0.02	-30.5 ± 1.5***
	500-nm	500	1620.7 ± 188.8*	0.66 ± 0.08	-28.3 ± 0.6**
	COOH-50	50	3735.0 ± 443.8**	0.48 ± 0.01	-13.8 ± 0.8***
	Plain-50	50	5951.0 ± 264.3***	0.60 ± 0.05	-31.3 ± 4.4**
	NH_2-50	50	96.5 ± 2.0***	0.52 ± 0.01	15.6 ± 2.7***

748

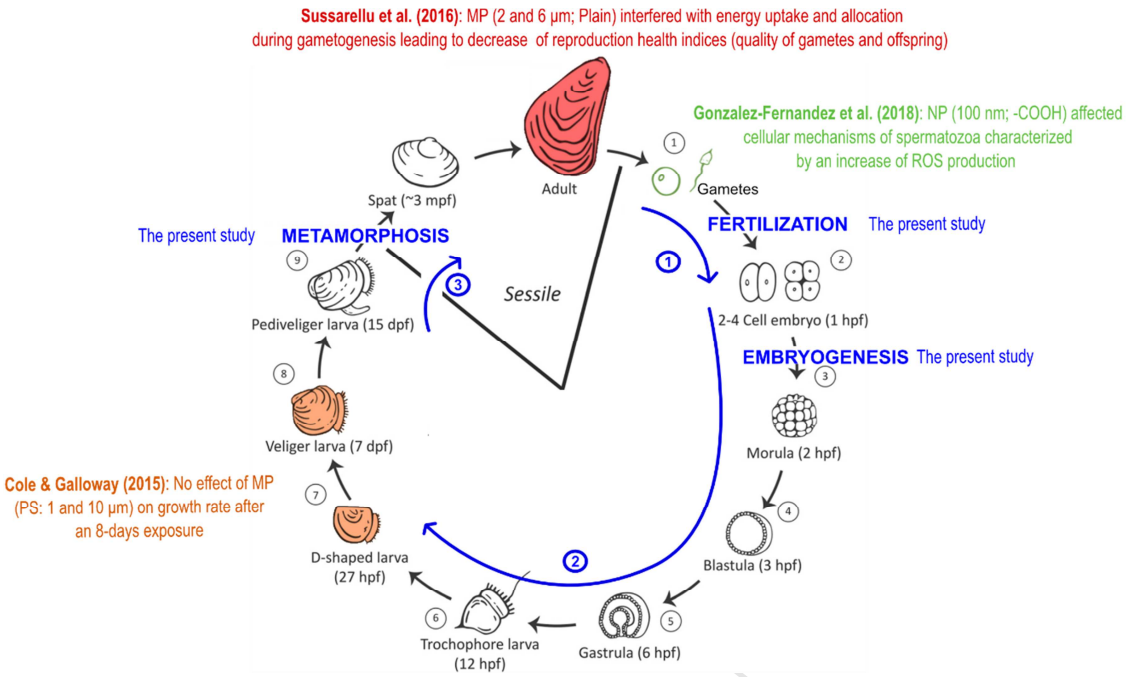

Fig. 1

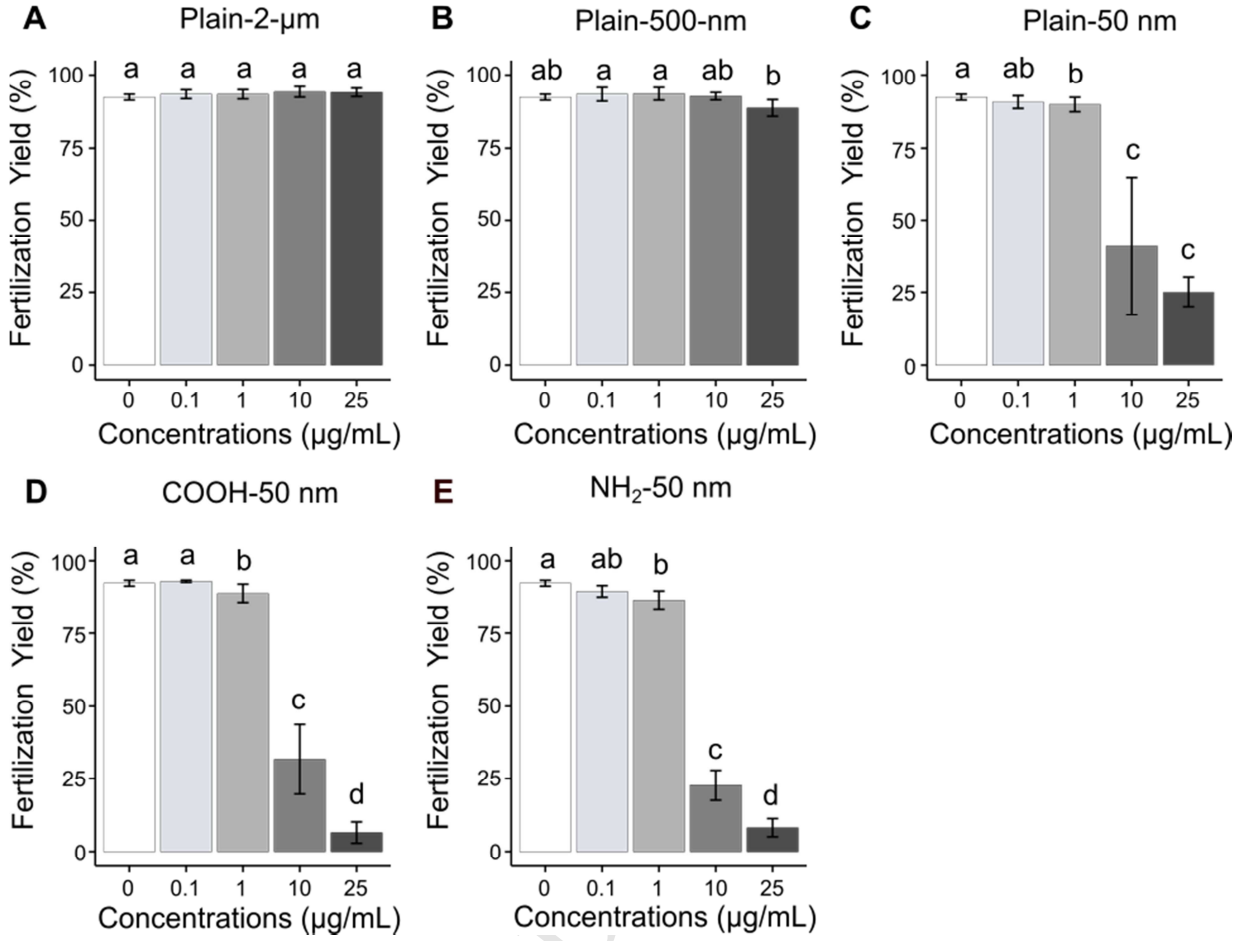

Fig. 2

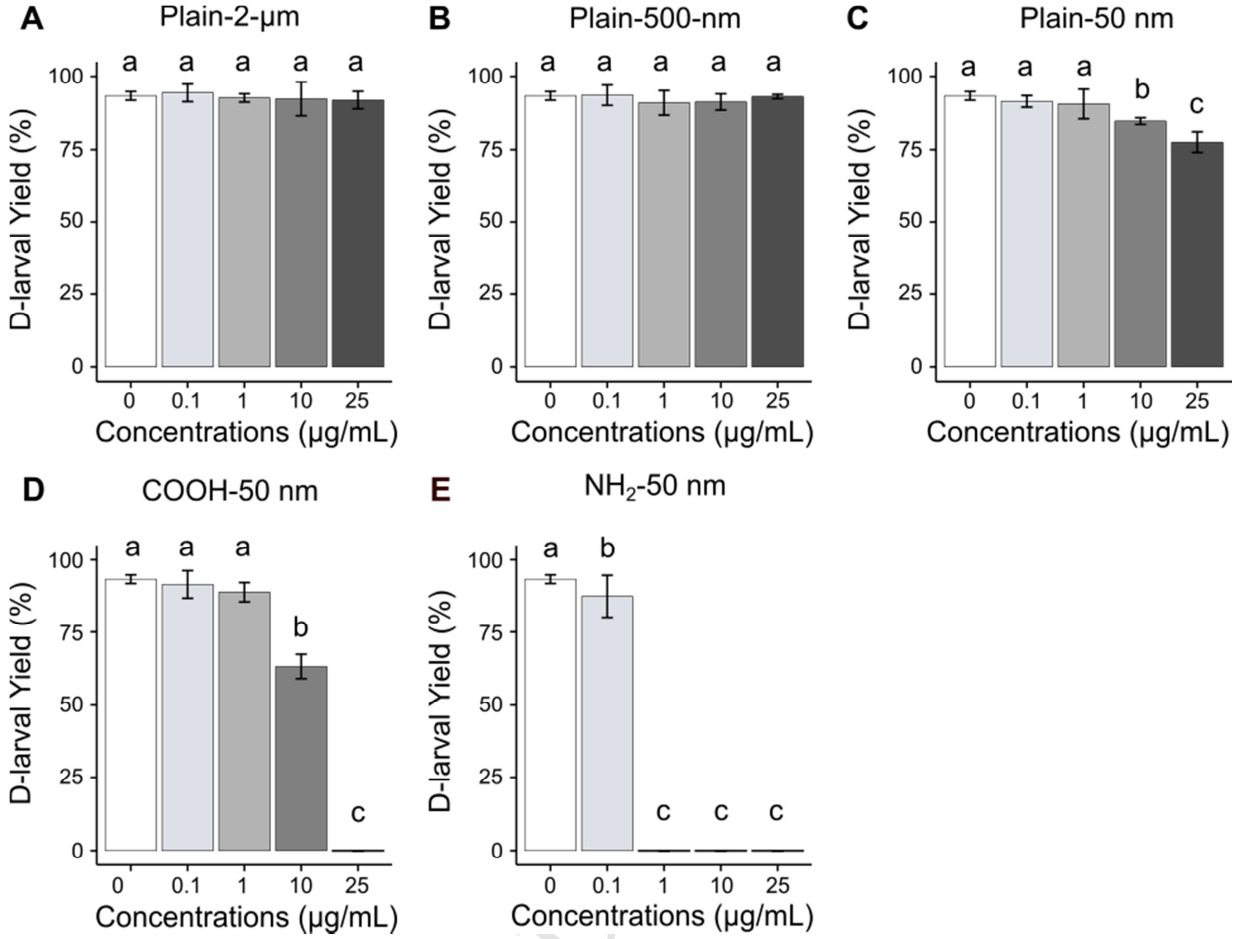

753

754 **Fig. 3**

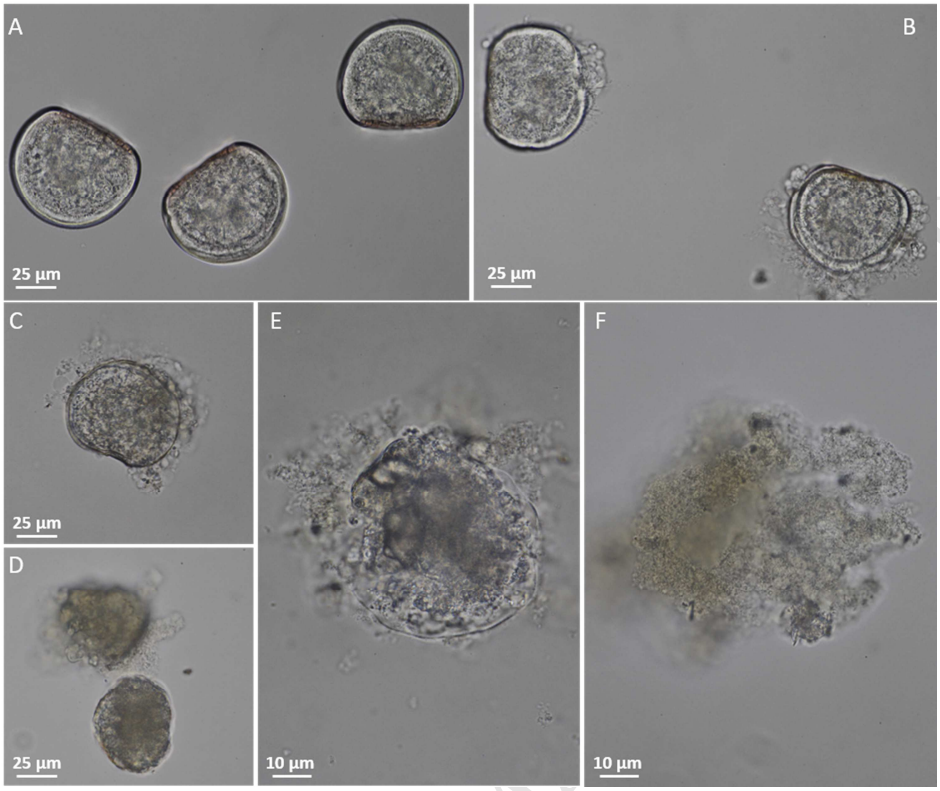

Fig. 4